

Timing jitter smoothing by Talbot effect.

I. Variance

Carlos R. Fernández-Pousa and Felipe Mateos

División de Óptica, Departamento de Ciencia y Tecnología de Materiales, Universidad Miguel Hernández, Avenida Ferrocarril s/n, E03202 Elche (Alicante) Spain

Laura Chantada, María Teresa Flores-Arias, Carmen Bao, María Victoria Pérez, and Carlos Gómez-Reino

Grupo de Óptica GRIN, Departamento de Física Aplicada, Universidade de Santiago de Compostela, Campus Sur, E15782 Santiago de Compostela, Spain

Received February 14, 2003; revised manuscript received June 20, 2003; accepted July 24, 2003

A study of the stochastic description of the Talbot effect in the temporal domain under random timing jitter is presented. The relevant statistical quantity is the variance. The variance of a train of pulses, each one affected by random timing jitter, shows peaks in the edges of the pulses. When this train is Talbot-imaged, the variance becomes flattened along the unit interval corresponding to each pulse as a result of the dispersion of the individual pulses of the train. Fractional Talbot devices are also analyzed. In particular, it is shown that this smoothing effect also occurs in Talbot devices leading to $N \times$ repetition rates of the original train.

© 2004 Optical Society of America

OCIS codes: 030.1670, 070.6760, 320.5550, 060.2340.

1. INTRODUCTION

The Talbot effect is widely known as a coherent phenomenon in the paraxial diffraction region after a grating.^{1,2} Basically, it consists in the repetition of the periodic structure of the grating in specific locations along the optical axis, as a result of the coherent interference of the diffraction orders of the grating. In this sense, it is a collective phenomenon, since the resulting pattern is a consequence of the whole periodic structure of the grating. This spatial effect has been demonstrated and applied not only in free space, but in inhomogeneous media³ and in waveguides,⁴ where the modes of the waveguide play the same role as the diffraction orders of the grating.

It has been noted⁵⁻⁷ that the same phenomenon is easily produced in the temporal domain by use of a highly dispersive medium. This observation is a consequence of the well-known analogy⁸ between the mathematics describing one-dimensional paraxial diffraction and pulse propagation in a linear, dispersive guiding medium with negligible attenuation. In this analogy, the pulse envelope is equivalent to the complex amplitude distribution of light in diffractive optics, dispersion is equivalent to diffraction, and the periodicity of the train of pulses is equivalent to the periodicity of the grating. In Ref. 6 it was shown that simple devices, such as a linearly chirped fiber grating (LCFG) or a high dispersion fiber, are suitable for constructing a Talbot device in the temporal domain. The group-velocity dispersion coefficient of the device is adjusted to produce a certain Talbot image of an incoming pulse train with a given period in exactly the same way that Talbot images are visualized by placing a screen after the grating in the appropriate positions.

One of the applications of the temporal Talbot effect is

to produce pulse trains of high frequency.^{6,7} Temporal Talbot devices of this type that use a linearly chirped fiber grating have been demonstrated in Ref. 7 that achieve repetition rates of $16\times$ of a train of pulses of 2.5 GHz to get a total rate of 40 GHz. It has also been proposed to use the temporal Talbot effect to measure dispersion parameters in fibers and other optic devices,⁹ and demonstrations of a fiber laser that uses this effect have been reported.¹⁰

In this paper we report on a basic characteristic of the Talbot effect, which is the stochastic variations of the central locations of the basic period. It seems natural that a collective effect would show some kind of stability under small variations of the parameters that define it. In this regard, the study presented here is suitable both for diffractive optics and for temporal optics. Here we will use the second point of view. In diffractive optics, stability of the Talbot effect under a set of deterministic variations¹ such as localized modifications of the basic period has been studied. The degradation of the effect due to the finite width of the grating and to the walk-off of the diffraction orders from the optical axis is also known. This walk-off effect progressively reduces the paraxial region where the Talbot effect takes place. In the temporal domain the study of the degradation by the finite width of the pulse trains has recently been addressed,¹¹ as has the stability of the Talbot effect under amplitude and phase unbalance between pulses. But to the best of our knowledge, no studies on stochastic variations have been reported, either in the spatial or the temporal domain.

Here we study the Talbot effect in the temporal domain under stochastic variations of the position of the pulses in a train. In temporal language, this amounts to random

timing jitter. Our result can be stated as follows: As a result of random jitter, pulses suffer large variations in certain positions of the unit interval assigned to each pulse. To be precise, the edges of the pulses have a larger variance than the peaks and valleys. After Talbot imaging, the variance is flattened along the unit interval. Thus, random jitter in the temporal domain is smoothed along each period. This phenomenon is different from other approaches describing the reduction of timing jitter in pulse trains, where jitter is decreased individually for each pulse (see, for instance, Ref. 12 and references therein), but shares with them the aim of exploring retiming procedures at the purely optical level.

The plan of the paper is the following. In Section 2 we state the problem in stochastic language. This will allow us to introduce the notation, which closely follows that of Ref. 13. The basic features of the Talbot effect are also briefly revisited. In Section 3 we present the computation of the variance of the pulse envelopes for arbitrary dispersion. Two limiting cases corresponding to input and output train variances after a pass through a Talbot device are analyzed. For both, approximate formulas are given. In Section 4 we present numerical simulations of the second Talbot plane that reproduces the original train of pulses. In Section 5 we analyze a fractional Talbot plane corresponding to a $4\times$ repetition rate. In particular, we show that the flattening of the variance is general for fractional Talbot devices leading to $N\times$ repetition rates. Finally, we present our conclusions in Section 6.

2. STOCHASTIC DESCRIPTION OF THE TALBOT EFFECT

Let us consider pulse propagation in linear dispersive media carried by quasi-monochromatic waves with central frequency ω_0 . The basic equation governing the propagation of the complex pulse envelope $x(z, t)$ in a dispersive medium along a distance z with negligible attenuation is¹⁴

$$\frac{\partial x}{\partial z} = -i \frac{\beta_2}{2} \frac{\partial^2 x}{\partial t^2}, \quad (1)$$

where $\beta(\omega) = \beta_0 + (\omega - \omega_0)\beta_1 + (\omega - \omega_0)^2\beta_2/2 + \dots$ is the expansion of the dispersion relation about the carrier frequency, and t is the time measured in the proper reference frame of the pulse, $t = t_{\text{phy}} - \beta_1 z$, with t_{phy} being the physical time. β_3 and other higher-order dispersion terms will not be taken into account. Then Eq. (1) is formally equivalent to the equation describing paraxial diffraction in one dimension, and the corresponding analogy is the basis for space-time duality between one-dimensional paraxial diffraction and pulse propagation in dispersive media.

The impulse response or propagation kernel of the linear system of Eq. (1) is simply the one-dimensional Fresnel diffraction kernel. For a dispersive medium of length L , this kernel is

$$h_\xi(t - t') = (-2\pi i \xi)^{-1/2} \exp[-i(t - t')^2/2\xi], \quad (2)$$

where $\xi = \beta_2 L$. General dispersive media with first-order dispersion, such as linearly chirped fiber gratings,

are characterized by the global parameter ξ with dimension T^{-2} , which represents the total dispersion of the device. In general, dispersive devices have a constant second-order parameter ξ only along a certain passband around the carrier frequency. In our analysis we will assume that the total bandwidth of the train of pulses lies inside this passband, so that ξ can be assumed constant for all frequencies.

A train of pulses $x_0(t)$ will be considered as the input field in a dispersive device described by Eq. (2):

$$x_0(t) = \sum_{k=-\infty}^{+\infty} f_0(t - kt_0 - a_k). \quad (3)$$

The function f_0 is the pulse form, which for simplicity will be considered as Gaussian with rms width equal to t_p and normalized in amplitude to unity,

$$f_0(t) = (2\pi t_p^2)^{-1/2} \exp(-t^2/2t_p^2). \quad (4)$$

Note that with this choice, the dimensions of the input field $x_0(t)$ are the inverse of time. The center of this train of pulses occurs at $t_k = kt_0 + a_k$. The set of variables a_k ($k = -\infty, \dots, +\infty$) is an infinite collection of random numbers with dimensions of time representing the timing jitter of each pulse. If the random numbers are set to zero, the train of pulses has a period of t_0 . We will assume that the pulse widths are smaller than this exact period, $t_p < t_0$, so that no overlapping between pulses occurs in the input train. We will consider that the random variables a_k are mutually independent, and its probability density function is Gaussian with zero mean and standard deviation t_j :

$$p(a_k) = (2\pi t_j^2)^{-1/2} \exp(-a_k^2/2t_j^2). \quad (5)$$

We will also assume that the jitter parameter t_j is smaller than the pulse width, $t_j < t_p$. The average over all the realizations of each one of jitter parameters a_k will be denoted with brackets, $\langle \dots \rangle$. Then, independence of timing variations implies that $\langle g(a_k)h(a_p) \rangle = \langle g(a_k) \rangle \langle h(a_p) \rangle$ when $k \neq p$ for any functions g and h .

The input field of Eq. (3) is transformed by the linear system of Eq. (2) into an output field $x_\xi(t)$ characterized by the dispersion parameter ξ :

$$x_\xi(t) = \int_{-\infty}^{+\infty} h_\xi(t - t') x_0(t') dt'. \quad (6)$$

Analogously, the output can be expressed as the coherent interference of a train of dispersed pulses:

$$\begin{aligned} x_\xi(t) &= \sum_{k=-\infty}^{+\infty} f_\xi(t - kt_0 - a_k) \\ &= \sum_{k=-\infty}^{+\infty} \int_{-\infty}^{+\infty} h_\xi(t - t') f_0(t' - kt_0 - a_k) dt', \end{aligned} \quad (7)$$

from which, by using Eqs. (2) and (4), the dispersed pulse is

$$f_\xi(t - kt_0 - a_k) = (2\pi\rho)^{-1/2} \exp[-(t - kt_0 - a_k)^2/2\rho], \quad (8)$$

with $\rho = t_p^2 - i\xi$.

Averaged fields can be computed in the time domain as follows. The mean envelope is a sum of averaged individual pulses, or the result of the propagation through the linear system of the initial averaged field:

$$\begin{aligned}\langle x_\xi(t) \rangle &= \sum_{k=-\infty}^{+\infty} \langle f_\xi(t - kt_0 - a_k) \rangle \\ &= \int_{-\infty}^{+\infty} h_\xi(t - t') \langle x_0(t') \rangle dt.\end{aligned}\quad (9)$$

A simple computation of the averaged dispersed field yields

$$\begin{aligned}\langle f_\xi(t - kt_0 - a_k) \rangle &= \int_{-\infty}^{+\infty} da_k p(a_k) f_\xi(t - kt_0 - a_k) \\ &= (2\pi\tilde{\rho})^{-1/2} \exp[-(t - kt_0)^2/2\tilde{\rho}],\end{aligned}\quad (10)$$

where we have introduced the notation $\tilde{\rho} = t_p^2 + t_j^2 - i\xi$. On the other hand, the initial averaged field is recovered by setting $\xi = 0$ in the value of $\tilde{\rho}$ in Eqs. (9) and (10). The result is a periodic train of pulses with enlarged rms width $\tilde{t}^2 = t_p^2 + t_j^2$,

$$\langle x_0(t) \rangle = \sum_{k=-\infty}^{+\infty} \tilde{f}_0(t - kt_0), \quad (11)$$

where

$$\tilde{f}_0(t) = (2\pi\tilde{t}^2)^{-1/2} \exp(-t^2/2\tilde{t}^2). \quad (12)$$

Thus, the averaged input field is affected by random jitter only as a temporal spreading of the initial pulses. The computation and interpretation of the output field is similar to a deterministic signal, and the details of the computation of Eq. (9) that result in the Talbot effect are widely known.^{1,2,15} Here we will simply quote the results.

The Talbot effect arises when the dispersion parameter is a fraction of a basic scale:

$$\xi = \frac{t_0^2}{2\pi} \frac{\gamma}{\alpha} \quad (13)$$

where γ and α are positive and coprime integers. When α is one, the Talbot effect is called integer, and the output is a replica of the original train of pulses for γ even and a replica of the original train, shifted by half a period, for γ odd. There is a simple proof of these facts in the Fourier domain. The transfer function of the linear system of Eq. (2) is $H_\xi(\omega) = \exp(i\xi\omega^2/2)$. On the other hand, for an exact periodic train of period t_0 , the spectral content of the input field consists of a set of delta functions at $\omega = 2\pi k/t_0$, with k integer. The transfer function for these frequencies reduces to $H_\xi(2\pi k/t_0) = \exp(i\pi\gamma k^2) = (-1)^{\gamma k}$. Then, the Talbot effect maintains the spectral components for γ even and adds a relative phase shift of π for γ odd. This phase shift is equivalent to a temporal shift of half a period in the time domain.

In diffractive optics, time harmonics correspond to diffraction orders. Therefore, the integer Talbot effect can be viewed as a coherent superposition of diffraction orders with in-phase or out-of-phase coincidence. The Talbot ef-

fect can also be interpreted as the result of the coherent interference of a periodic pattern of diffracted beams, each corresponding to the unit cell of the grating. In the temporal domain, this is equivalent to considering the interference of the basic pulses in the original train, highly dispersed after the Talbot device. In this paper we will mainly follow this second point of view.

When α in Eq. (13) differs from unity, the effect is called fractional Talbot or sub-Talbot. The output field in this case has a richer structure. It is again a periodic train of pulses with period t_0 shifted for odd γ . But the unit interval is composed of the coherent sum of α replicas of the original pulse shifted mutually by t_0/α , with power reduced by $1/\alpha$, and with definite phase differences between them. In diffractive optics, these α replicas constitute the unit cell of the Talbot-imaged grating. Repetition rates of the original train of pulses with rate $N\times$ can be obtained from $\gamma/\alpha = 1/N$ if the initial pulses are small enough to avoid superposition of neighboring pulses in each unit interval or unit cell. Finally, note the high dispersion scale of the transforming devices as given by Eq. (13). For instance, for a 10-GHz repetition rate, the first integer Talbot system requires a dispersion of $\xi = 1592 \text{ ps}^2/\text{rad}$. For $N\times$ repetition rates, the Talbot effect requires smaller dispersion, but always in the range of $10^3 \text{ ps}^2/\text{rad}$ for trains in the GHz range.

3. COMPUTATION OF THE VARIANCE

We are interested in the statistical variations of a concrete realization of a train of pulses affected by timing random jitter, rather than in mean values. To characterize them, it is necessary to calculate the corresponding variance. This quantity is defined as the averaged squared deviation of the field with respect to the mean for each temporal instant:

$$\begin{aligned}V_\xi(t) &= \langle |x_\xi(t) - \langle x_\xi(t) \rangle|^2 \rangle \\ &= \langle x_\xi(t)x_\xi(t)^* \rangle - \langle x_\xi(t) \rangle \langle x_\xi(t)^* \rangle,\end{aligned}\quad (14)$$

and it has the usual interpretation as a measure of the variation of the output field at each sampling instant. Expressed as a coherent sum of dispersed pulses, Eq. (7), the variance is

$$\begin{aligned}V_\xi(t) &= \sum_{k,m=-\infty}^{+\infty} \langle f_\xi(t - kt_0 - a_k) f_\xi(t - mt_0 - a_p)^* \rangle \\ &\quad - \left| \sum_{k=-\infty}^{+\infty} \langle f_\xi(t - kt_0 - a_k) \rangle \right|^2.\end{aligned}\quad (15)$$

By using the independence of the variables a_k , this expression can be easily cast as a sum over dispersed pulses:

$$\begin{aligned}V_\xi(t) &= \sum_{k=-\infty}^{+\infty} [\langle |f_\xi(t - kt_0 - a_k)|^2 \rangle \\ &\quad - |\langle f_\xi(t - kt_0 - a_k) \rangle|^2],\end{aligned}\quad (16)$$

where the first part of the sum corresponds to the averaged square of each dispersed pulse and the second to the square of the average. It is a simple task to compute

both contributions. The result is the difference of two trains of Gaussian functions:

$$V_\xi(t) = \frac{1}{t_p \sqrt{4\pi}} \sum_{m=-\infty}^{+\infty} \frac{1}{\eta_1(\xi) \sqrt{2\pi}} \exp\left[-\frac{(t - mt_0)^2}{2\eta_1^2(\xi)}\right] - \frac{1}{\bar{t} \sqrt{4\pi}} \sum_{s=-\infty}^{+\infty} \frac{1}{\eta_2(\xi) \sqrt{2\pi}} \exp\left[-\frac{(t - st_0)^2}{2\eta_2^2(\xi)}\right], \quad (17)$$

where we have introduced the following notations:

$$\eta_1^2(\xi) = \frac{\xi^2 + t_p^2 \bar{t}^2}{2t_p^2}, \quad \eta_2^2(\xi) = \frac{\xi^2 + \bar{t}^4}{2\bar{t}^2}, \quad (18)$$

and $\hat{t}^2 = \bar{t}^2 + t_j^2 = t_p^2 + 2t_j^2$. Then the width $\eta_1(\xi)$ represents the rms widths of the averaged squared dispersed pulses, and $\eta_2(\xi)$ denotes the rms width of the square of the average dispersed pulse. Therefore, variance is composed of two contributions coming from individual dispersed pulses, which will be called of $\langle |f|^2 \rangle$ and $|\langle f \rangle|^2$ type, respectively. Since $V_\xi(t)$ is a periodic series, it can also be expanded in a Fourier series of the form

$$V_\xi(t) = \sum_{m=-\infty}^{+\infty} g_m \exp(2\pi i m t / t_0) = g_0 + 2g_{\pm 1} \cos(2\pi t / t_0) + \dots \quad (19)$$

with $g_m = g_{-m}$ and

$$g_m = \frac{1}{t_0 t_p \sqrt{4\pi}} \exp[-2\pi^2 m^2 \eta_1^2(\xi) / t_0^2] - \frac{1}{t_0 \bar{t} \sqrt{4\pi}} \exp[-2\pi^2 m^2 \eta_2^2(\xi) / t_0^2]. \quad (20)$$

Both forms of the variance, Eqs. (17) and (19), will be used in what follows. From Eq. (19) it is worth noting that

$$\frac{1}{t_0} \int_{-t_0/2}^{t_0/2} V_\xi(t) dt = g_0 = \frac{1}{t_0 \sqrt{4\pi}} \left(\frac{1}{t_p} - \frac{1}{\bar{t}} \right), \quad (21)$$

that is, the mean value is constant and there is no dependence on the specific value of the dispersion parameter ξ .

The variance of the input field $V_0(t)$ can be recovered by setting $\xi = 0$ in Eq. (17) through the corresponding values of the widths, Eq. (18). Since the jitter parameter is small compared with the width of the original pulses, $t_j < t_p$, both widths become of the order of the original pulses, $\eta_1(0), \eta_2(0) \approx t_p$. Moreover, since the pulses do not overlap, only two Gaussian functions contribute appreciably to $V_0(t)$ in the sum Eq. (17) for each unit interval. For instance, for the central period $-t_0/2 < t < t_0/2$, the following approximation applies:

$$V_0(t) \cong \langle |f(t - a_0)|^2 \rangle - |\langle f(t - a_0) \rangle|^2 = \frac{1}{\sqrt{8\pi^2}} \left[\frac{1}{t_p \eta_1(\xi)} \exp\left(-\frac{t^2}{2\eta_1^2(\xi)}\right) - \frac{1}{\bar{t} \eta_2(\xi)} \exp\left(-\frac{t^2}{2\eta_2^2(\xi)}\right) \right]. \quad (22)$$

On the other hand, the variance of the output envelope cannot be approximated in this way: when ξ is different from zero, the dispersed widths [Eq. (18)] are larger than t_0 , and then the Gaussian functions in Eq. (17) overlap between adjacent periods. Indeed, for a general Talbot condition, Eq. (13), the first of these widths is

$$\eta_1^2(\xi) = \frac{t_0^2 t_0^2 \gamma^2}{8\pi^2 t_p^2 \alpha^2} + \frac{\hat{t}^2}{2}. \quad (23)$$

The first term in this sum dominates over the second by virtue of the ratio t_0^2/t_p^2 . This width is, in general, of the order of the period of the pulses, $\eta_1(\xi) \approx t_0$, at least for $\gamma/\alpha \geq 1$. The same argument applies for $\eta_2^2(\xi)$, resulting also in $\eta_2(\xi) \approx t_0$. In order to obtain a simpler expression for the variance $V_\xi(t)$ after the dispersive device, it is necessary to return to the Fourier expansion (19), whose coefficients are given in Eq. (20). Now, since $\eta_1(\xi), \eta_2(\xi) \approx t_0$, all harmonics in this expansion are damped. The leading-order approximation is just the DC term:

$$V_\xi(t) \cong g_0. \quad (24)$$

This, together with Eq. (21), means that the output variance equals the mean value along the unit interval, and it is insensitive to ξ .

In Fig. 1 we present the central pulse contributions $\langle |f|^2 \rangle$ and $|\langle f \rangle|^2$ to input and output variances in an example. The parameters are the same as those in Section 5 below. The period has been chosen as $t_0 = 1$ in suitable units; then, the central unit interval is $-0.5 < t < 0.5$. Moreover, $\gamma/\alpha = 1/4$, $t_p = 0.050$, and $t_j = 0.020$. We have chosen a rather large jitter coefficient

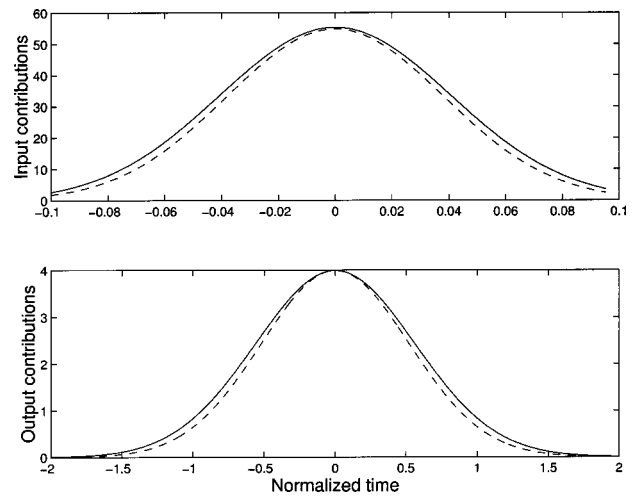


Fig. 1. Contributions of type $\langle |f|^2 \rangle$ (solid curve) and $|\langle f \rangle|^2$ (dashed curve) to the input (top graph) and output (bottom graph) variances due to a single pulse.

to emphasize the effect. Although a detailed analysis of this example should wait until Section 5, we present the result here to visualize the smoothing effect and discuss its physical basis. In the upper part of the plot, the initial contributions are contained in a single unit interval, so that they do not overlap with neighboring intervals. Moreover, their difference is large, so the variance $V_0(t)$ can be approximated to its difference, neglecting contributions from other pulses, as in Eq. (22). In the lower part we show these contributions after the dispersive device. Both have been broadened by dispersion, they overlap with other intervals, and their difference is smaller. Therefore, all the pulses in the output train of Eq. (17) must be added to give an approximation of the variance. The leading term in the approximation is the DC term, Eq. (24). Then, the dual behavior of the variance is a consequence of the dispersion of the individual pulses that smooth the difference between contributions $\langle |f|^2 \rangle$ and $|\langle f \rangle|^2$. In conclusion, the output variance is approximately constant. This conclusion remains valid as long as $\eta_1(\xi)$, $\eta_2(\xi) \approx t_0$ because of the truncation of the series of Eq. (19). However, for small-dispersion systems, or equivalently, for values of the Talbot index $\gamma/\alpha < 1$, the approximation may fail. This fact will be analyzed in Section 5.

4. INTEGER TALBOT DEVICES

Here we will consider the second integer Talbot condition, characterized by $\gamma/\alpha = 2$, as an example. The output train of pulses is an exact replica of the original one if jitter is absent. Our computations in the preceding paragraphs assume an infinite sequence of incoming pulses. To avoid the walk-off effect, a sufficiently long train of pulses has been considered in the simulations, and statistical analysis is carried out in the central region of the output trains.

A sequence of 200 Gaussian pulses was generated. The exact repetition period was normalized to unity, $t_0 = 1$. The Gaussian functions describing the pulses had a rms width of $t_p = 0.100$, and random jitter was added following a distribution with standard deviation of $t_j = 0.015$. Each of the unit intervals was sampled with 128 points. The results of the simulation are represented in Figs. 2–5. In Fig. 2, the ten central unit intervals are shown for the input train of pulses (above) and for the output train (below). We observe the presence of signal in the space between pulses, an unusual feature compared with the exact Talbot effect. Moreover, differences between the heights of pulses are also clear.

To show the smoothing effect, we superimposed ten unit intervals from the central section of the pulse trains. In Fig. 3 we show the result for the input train and in Fig. 4 for the output train. In the first case, the edges of the pulses are displaced by random jitter. Assuming that statistical averages can be inferred from temporal averages, this means that for instants of time in the edges of the pulse, the variance of the process is high. In contrast, variations of the central peak and of the valleys between pulses are small, resulting in a small variance. The plot of the superposition of output pulses in Fig. 4 is different. Clearly, the edges present small variations,

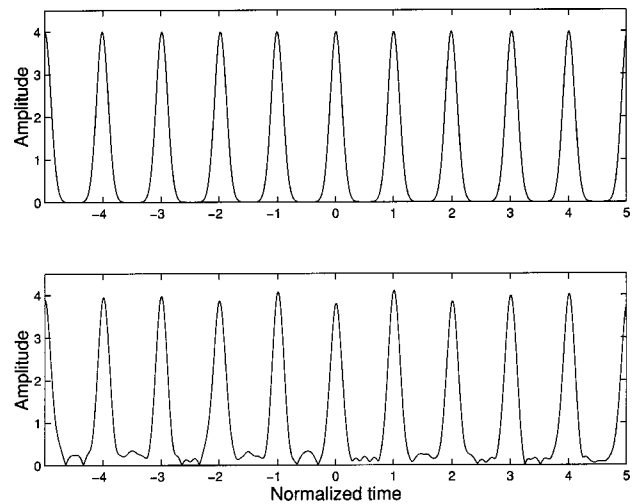


Fig. 2. Ten central unit intervals of the input (top) and output trains of pulses (bottom) in the integer Talbot device characterized by the index $\gamma/\alpha = 2$. The rms width of the input pulses is $t_p = 0.100$ and the standard deviation of random timing jitter is $t_j = 0.015$.

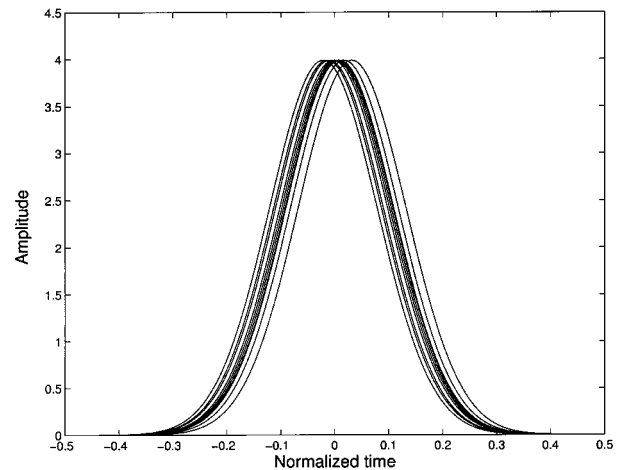


Fig. 3. Superposition of ten input pulses in a unit interval in the integer Talbot device characterized by the index $\gamma/\alpha = 2$. Parameters as in Fig. 2.

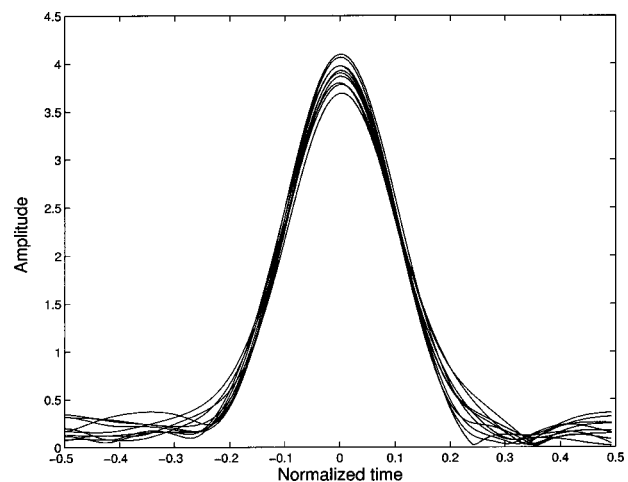


Fig. 4. Superposition of ten output pulses in a unit interval in the integer Talbot device characterized by the index $\gamma/\alpha = 2$. Parameters as in Fig. 2.

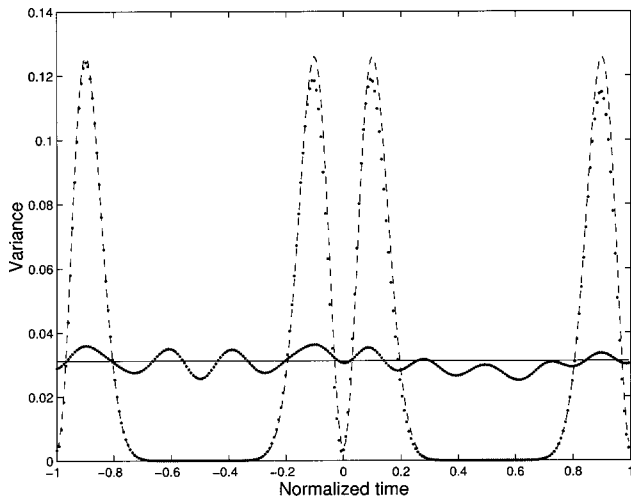


Fig. 5. Input variance in two unit intervals obtained from Eq. (22) (dashed curve) and through a numerical estimate over 100 sample trains (dots); output variance for $\gamma/\alpha = 2$ in two unit intervals obtained from Eq. (24) (solid line) and through a numerical estimation (dots). Parameters as in Fig. 2.

but the corresponding variations in valleys and peaks are increased. This behavior is in accordance with our observations concerning Fig. 2.

The time variations of the pulse envelopes are described by the input and output variances $V_0(t)$ and $V_\xi(t)$. To get a numerical estimate of these quantities, a set of 100 processes, each containing 200 pulses with different individual jitter parameters but with the same standard deviation $t_j = 0.015$, was generated. Each of these experiments is described by the same set of parameters as before. We focused on the two central unit intervals, performing a point estimation of the variance for each of the 128 samples per period. The results are shown in Fig. 5, where both the input and output variances are shown. The double-peaked function corresponds to the input train and the flat one to the output.

The functions $V_0(t)$ and $V_\xi(t)$ have been evaluated from the exact expression of the variance as an infinite sum of pulses, Eq. (17). We note the good agreement between the estimate and the analytical formulas. The input and output approximations to the variance formula are not shown in this figure since they are indistinguishable from the result of Eq. (17). In particular, we note that the constant output variance given by Eq. (24) yields a value $V_\xi(t) = 0.031$, in accordance with the results of this simulation. Note that we have evaluated the variance in Fig. 5 as an average over independent trains, not as temporal averages over the periods of a single train. This means that no ergodic assumptions have been made. However, we have verified that estimates from averages over periods yield results analogous to those in Fig. 5.

5. $1/N$ FRACTIONAL TALBOT DEVICES

In this section we will focus on the series of Talbot devices characterized by indices $\gamma/\alpha = 1/N$. They are known to provide a way to generate trains of pulses with $N\times$ repetition rates with respect to the original train. Our first simulations deal with the Talbot dispersive device corre-

sponding to $\gamma/\alpha = 1/4$. Again, a train of 200 Gaussian pulses was generated, in this case with $t_p = 0.050$ and $t_j = 0.020$, the remaining parameters as before. The pulse width was reduced with respect to the value of Section 4 to show the $4\times$ repetition effect. In Fig. 6 we present the superposition in the same unit interval of ten sets of output unit intervals, each containing four slightly overlapped pulses. The variance of the pulses was also simulated with 100 trains of 200 pulses, and the estimates in the two central unit intervals are shown in Fig. 7. Again, we observe the initial double peak and the nearly flat output variance, with the same interpretation as in Section 4. The constant value of the output variance approximation of Eq. (24) is, in this case, 0.403, in accordance with the result of this simulation.

Although the constant value of the variance was a good approximation in this example, it was noted before that it

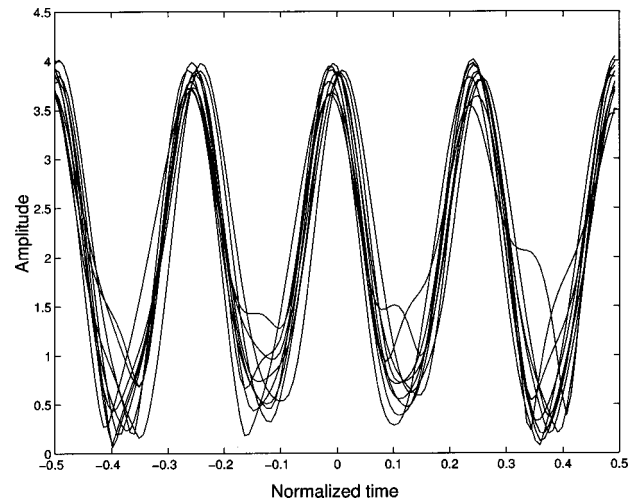


Fig. 6. Superposition of ten sequences of output pulses in a unit interval in the fractional Talbot device characterized by the index $\gamma/\alpha = 1/4$, leading to a $4\times$ repetition rate. The rms width of the input pulses is $t_p = 0.050$ and the standard deviation of random timing jitter is $t_j = 0.020$.

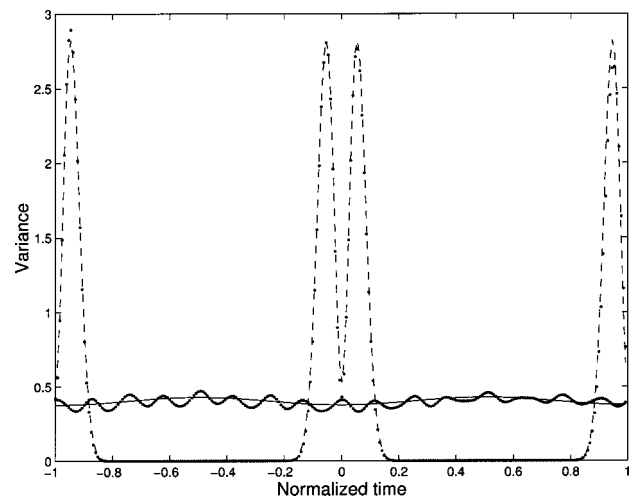


Fig. 7. Input variance in two unit intervals obtained from Eq. (22) (dashed curve) and through a numerical estimate over 100 sample trains (dots); output variance for $\gamma/\alpha = 1/4$ in two unit intervals obtained from Eq. (24) (solid curve) and through a numerical estimation (dots). Parameters as in Fig. 6.

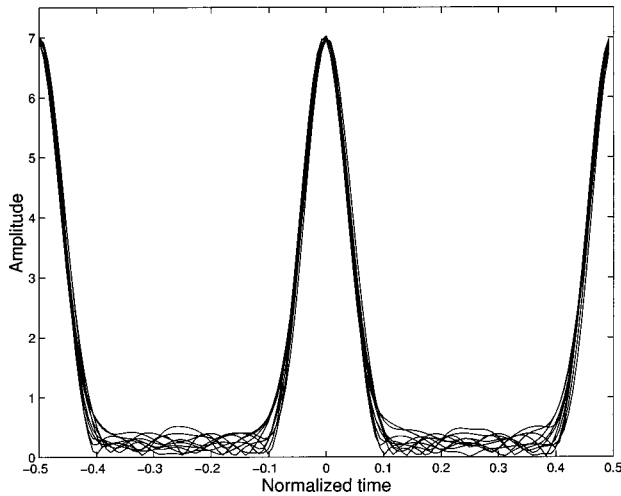


Fig. 8. Superposition of ten sequences of output pulses in a unit interval in the fractional Talbot device characterized by the index $\gamma/\alpha = 1/2$, leading to a $2\times$ repetition rate. The rms width of the input pulses is $t_p = 0.040$ and the standard deviation of random timing jitter is $t_j = 0.007$.

may fail when the Talbot index γ/α is sufficiently small. Here we will show that, for experiments designed to create high repetition rates, the output variance is still constant to a good approximation. The important observation is the following: Repetition rates of a given train are obtained if the individual pulses are narrow enough that they do not to overlap after the device. It is a simple task to quantify this observation for Gaussian pulses. We set as a criterion that overlapping is negligible when the midpoint between adjacent pulses has contributions in amplitude from both pulses that are not larger than $1/10$ of the peak value. For Gaussian pulses this means that the pulse width for this limiting condition is

$$\frac{t_p}{t_0} = \frac{1}{2N\sqrt{2 \ln 10}}. \quad (25)$$

With this convention we can compute the damping coefficients $2\pi^2\eta_1^2(\xi)/t_0^2$ and $2\pi^2\eta_2^2(\xi)/t_0^2$ of the first harmonic in expansion (19):

$$2g_{\pm 1} = \frac{\exp(-2\pi^2\eta_1^2(\xi)/t_0^2)}{t_0 t_p \sqrt{\pi}} - \frac{\exp(-2\pi^2\eta_2^2(\xi)/t_0^2)}{t_0 \bar{t} \sqrt{\pi}}. \quad (26)$$

Here we will focus only on the second one, which in this example is the smaller; see Fig. 1. Nevertheless, both have in general the same order of magnitude. This damping coefficient can be bounded for $\gamma/\alpha = 1/N$ as follows:

$$\begin{aligned} \frac{2\pi^2\eta_2^2(\xi)}{t_0^2} &= \frac{1}{4N^2} \frac{t_0^2}{t_p^2 + t_j^2} + \pi^2 \frac{t_p^2}{t_0^2} + \pi^2 \frac{t_j^2}{t_0^2} \\ &> \frac{1}{4N^2} \frac{t_0^2}{t_p^2 + t_j^2} > \frac{1}{8N^2} \frac{t_0^2}{t_p^2} \\ &= \ln 10, \end{aligned} \quad (27)$$

where we have used Eq. (13) and notations (18), and, in the last inequality, that $t_j < t_p$. Then, the value of $2\pi^2\eta_2^2(\xi)/t_0^2$ decreases as $1/N^2$, but since the ratio t_p/t_0 is also reduced by a factor N to avoid overlapping [see Eq. (25)], this damping coefficient is constant for any N . The value in Eq. (27) corresponds to a conservative damping factor of $\exp[-2\pi^2\eta_2^2(\xi)/t_0^2] \leq 0.10$. This results in a maximum modulation of the constant variance of 20%. The actual value of modulation is typically lower, especially if jitter is negligible. For the parameters presented here, with t_j and t_p of the same order, the modulation is of 6%. Numerical results in Fig. 7 illustrate these values. Thus, we conclude that when the sequence of pulses is sufficiently narrow to avoid overlapping in the fractional Talbot series, the contribution of higher-order harmonics to expression (24) is to a good approximation negligible. If overlapping is allowed such that the ratio t_p/t_0 is kept constant, the constant approximation fails as γ/α decreases.

A new feature appearing in this last simulation is the increase of pulse pedestal in fractional Talbot devices. This fact is obscured in Fig. 6 because of the overlapping between adjacent pulses. In Fig. 8 we present a new simulation for the fractional Talbot device corresponding to $\gamma/\alpha = 1/2$, with $t_p = 0.040$ and $t_j = 0.007$. The presence of pedestal here is clear. To analyze this feature, let us consider a general Talbot device characterized by an index γ/α . The repetition-rate series correspond to the fractional Talbot series $\gamma/\alpha = 1/N$. From Eq. (14) the power of the mean detected train $\langle x_\xi(t)x_\xi(t)^* \rangle$ is composed of the constant variance $V_\xi(t) = \sigma_\xi^2$ plus the squared mean train $\langle x_\xi(t) \rangle \langle x_\xi(t)^* \rangle$, which vanishes between pulses. In turn, the peak value of the output pulses in a general Talbot device is damped^{2,15} in amplitude by a factor of $1/\alpha^{1/2}$ with respect to the original train, Eq. (12). Then, for Gaussian pulses the ratio between the peak amplitude of the detected train (A_{peak}) to the value between pulses (σ_ξ) is

$$\begin{aligned} \frac{A_{\text{peak}}}{\sigma_\xi} &= \frac{((1/2\pi\alpha\bar{t}^2) + \sigma_\xi^2)^{1/2}}{\sigma_\xi} \\ &\cong \frac{1}{\sigma_\xi \bar{t} \sqrt{2\pi\alpha}} \cong \frac{\sqrt{2}}{\pi^{1/4}} \frac{1}{\sqrt{\alpha}} \left(\frac{t_p}{t_0}\right)^{1/2} \frac{t_0}{t_j}, \end{aligned} \quad (28)$$

where in the last approximation we have retained the leading order in the ratio t_j/t_p from Eq. (21). Therefore, for a given amount of jitter the pedestal increases as $\sqrt{\alpha} = \sqrt{N}$. Moreover, the ratio decreases when the input pulses are wider. For the simulation in Fig. 8, this ratio is 21.2, with $A_{\text{peak}} = 7$ and $\sigma_\xi = 0.33$.

6. CONCLUSIONS

In this paper we have studied the influence of random jitter in the Talbot effect. The analysis has been performed in the temporal domain. We have shown that the variance of the train of pulses is flattened by use of dispersion after passing a Talbot device. This is due to the dispersion of the individual pulses that form the train, as their variance is spread on neighboring intervals. We have also given approximate formulas for the input and output

variances and discussed the validity of these approximations. For integer Talbot devices, the value of the variance is constant irrespective of the value of the dispersion. For fractional Talbot devices with $\gamma/\alpha < 1$, a modulation of the constant value of the variance may be present, depending on the ratio between the pulse width and the period of the original train. Nevertheless, for Talbot devices leading to $N \times$ repetition rates, the variance still is, to a good approximation, constant. The presence of pulse pedestal in these devices has also been analyzed.

ACKNOWLEDGMENTS

This work has been supported by Ministerio de Ciencia y Tecnología, Spain, under contract TIC2003-03041. The research of M. T. Flores-Arias was supported by the government of Spain through a Formación Personal Investigador (FPI) grant. The authors wish to thank the referees of this paper for their useful comments, which helped us to improve the content.

Corresponding author C. R. Fernández-Pousa may be reached by e-mail to c.pousa@umh.es.

REFERENCES

1. K. Paturski, "The self-imaging phenomenon and its applications," in *Progress in Optics, Vol. XXVII*, E. Wolf, ed. (Elsevier, Amsterdam, 1989), pp. 1–108.
2. M. V. Berry and S. Klein, "Integer, fractional, and fractal Talbot effects," *J. Mod. Opt.* **43**, 2139–2164 (1996).
3. M. T. Flores-Arias, C. Bao, M. V. Pérez, and C. R. Fernández-Pousa, "Fractional Talbot effect in a Selfoc gradient-index lens," *Opt. Lett.* **27**, 2064–2066 (2002).
4. R. Ulrich, "Image formation by phase coincidences in optical waveguides," *Opt. Commun.* **13**, 259–264 (1975).
5. T. Jansson and J. Jansson, "Temporal self-imaging in single-mode fibers," *J. Opt. Soc. Am.* **71**, 1373–1376 (1981).
6. J. Azaña and M. A. Muriel, "Technique for multiplying the repetition rates of periodic trains of pulses by means of a temporal self-imaging effect in chirped fiber gratings," *Opt. Lett.* **24**, 1672–1674 (1999).
7. S. Longhi, M. Marano, P. Laporta, O. Svelto, M. Belmonte, B. Agogliati, L. Arcangeli, V. Pruneri, M. N. Zervas, and M. Ibsen, "40-GHz pulse-train generation at 1.5 μm with a chirped fiber grating as a frequency multiplier," *Opt. Lett.* **25**, 1481–1483 (2000).
8. A. Papoulis, "Pulse compression, fiber communications and diffraction: a unified approach," *J. Opt. Soc. Am. A* **11**, 3–13 (1994).
9. J. Azaña and M. A. Muriel, "Temporal Talbot effect in fiber gratings and its applications," *Appl. Opt.* **38**, 6700–6704 (2000).
10. B. Fischer, B. Vodonos, S. Atkins, and A. Bekker, "Dispersion-mode pulsed laser," *Opt. Lett.* **25**, 728–730 (2000).
11. J. Azaña, "Temporal self-imaging effects for periodic optical pulse sequences of finite duration," *J. Opt. Soc. Am. B* **20**, 83–90 (2003).
12. L. E. Jiang, M. E. Grein, H. A. Haus, E. P. Ippen, and H. Yokohama, "Timing jitter eater for optical pulse trains," *Opt. Lett.* **28**, 78–80 (2003).
13. A. Papoulis, *Probability, Random Variables and Stochastic Processes*, 2nd ed. (McGraw-Hill, New York, 1984).
14. G. P. Agrawal, *Nonlinear Fiber Optics*, 3rd ed. (Academic, Boston, 2001).
15. C. Gómez-Reino, M. V. Pérez, and C. Bao, *Gradient-Index Optics: Fundamentals and Applications* (Springer-Verlag, Berlin, 2002), Chap. 7.